Defect Dependent Elasticity: Nanoindentation as a Probe of Stress-State

K.F. Jarausch, North Carolina State University, Raleigh NC.
J.D. Kiely, Sandia National Laboratories, Albuquerque NM.
J.E. Houston, Sandia National Laboratories, Albuquerque NM.
P.E. Russell, North Carolina State University, Raleigh NC.

Abstract

Nanoindentation studies reveal that the measured elastic properties of materials can be strongly dependent upon their stress-state and defect structure. Using an interfacial force microscope (IFM), the measured elastic response of 100 nm thick Au films was found to be strongly correlated with the films' stress state and thermal history. Indentation elasticity was also found to vary in close proximity to grain boundaries in thin films and near surface steps on single crystal surfaces. Molecular dynamics simulations suggest that these results cannot be explained by elasticity due only to bond stretching. Instead, the measured elastic properties appear to be a combination of bond and defect compliance representing a composite modulus. We propose that stress concentration arising from the structure of grains, voids and grain boundaries is the source of an additional compliance which is sensitive to the stress state and thermal history of a material. The elastic properties of thin metallic films appear to reflect the collective elastic response of the grains, voids and grain boundaries. These results demonstrate that nanoindentation can be useful as a highly localized probe of stress-state and defect structures.

1.0 Introduction

The determination of the mechanical properties of nanostructured materials is critical to the continuing development of thin film technology. In particular the correlation between mechanical response, stress state and deposition conditions have been documented for several materials but are not well understood [1,2]. Deformation properties unique to the nanoscale have been attributed to a material's high defect densities and to changes in the mechanisms accommodating deformation [2-10]. Such mechanical behavior has been observed in bulk samples with grain sizes below 10-20 nm for which a significant volume fraction of atoms reside in the intercrystalline grain boundary regions [3,4,7-10]. For thin films the constraints of film thickness, adhesion to the substrate and non-random texture extend the range of grain sizes over which such 'nanocrystalline' mechanical properties are observed [1,2,5,8]. The metallic thin films used as interconnects in integrated circuits are of particular technological relevance. These films are reported to be highly defected with large internal stresses [11-17] which contribute to their unique elastic and plastic properties [1,2]. These investigations suggest that the conventional measurement techniques and

DISCLAIMER

models used to describe the deformation of bulk materials are not always applicable to thin film systems.

While it has long been recognized that a material's plastic properties are controlled by its defects, a material's elastic properties are generally attributed to its bond character [18]. However, a few reports have suggested a link between structure and elastic response for some nanostructured materials. Such elastic properties have been attributed to intercrystalline regions with differing interatomic spacings [5,9,10,19,20], or potentials [20], and porosity [6,21,22,24]. In most cases the link between elastic response and structure was found to be highly dependent upon processing conditions. A variety of thin films (Al, Cu, Au, Au-Ni, Ag-Ni) deposited under non-equilibrium conditions [5,8,10,23] and nanocrystalline bulk materials (Cu, Pd, ZnO, CaF_2) [6,9,10,22,24] have exhibited large variations of hardness, elasticity and stress state as a function of processing. These reports suggest a link between measured elastic properties and defect structure.

A previous IFM study revealed that the deformation response of 200 nm thick Au films was dependent upon subsurface free volume [8] in the form of voids or underdense grain boundaries. A survey of individual grains demonstrated that the initial plastic response was accommodated by intergranular deformations. Grain to grain variations of the measured elastic modulus and shear-stress at yield were attributed to local differences in the subsurface free volume. More recently, the IFM was used to probe the elastic properties of Au films with smaller grain sizes (average grain diameter of 25-50 nm instead of 500nm) [25,26]. For these samples, measurements of elastic moduli were consistent from point to point and sample to sample for samples made with similar deposition conditions. However, large sample to sample variations were observed as a function of film adhesion-layer combination and substrate temperature during deposition. These variations were found to correlate with the samples' residual stress state and not with morphology or substrate adhesion [25,26].

LaFontaine et al. were the first to propose that nanoindentation might be used as a sensitive and highly localized probe of stress state [23]. They reported factor of two decreases of hardness accompanying the stress relaxation of 0.3 μm and 0.53 μm thick Al films (A correlation of elastic response and stress-state was not documented in these measurements). Suresh and Giankopolous [27] recently proposed an analytical model for the dependence of hardness upon stress state. Unfortunately, hardness measurements are only sensitive to large changes in stress state (>100 MPa) [27-29] and are inherently destructive. Tusi et al. performed a rigorous analysis of the dependence of nanoindentation response upon applied stress using coarse-grained polycrystalline aluminum alloy samples [28]. Their work verified the dependence of hardness upon stress but also showed a slight

variation of measured elastic modulus with applied stress. Subsequent analysis revealed that this sensitivity was due to an improper estimation of the contact areas during indentation as a result of pileup behavior [27].

This study is aimed at characterizing the elastic properties of Au thin films widely used as interconnects in GaAs integrated circuits. Understanding the response of these thin films and their dependence upon processing conditions is critical for device design and modeling. To this end, the elastic properties of 100 nm thick (blanket) Au films were studied as a function of an applied stress and thermal history. In an effort to document the link between measured elastic properties and defect structure, the thin film response was measured with a range of indenter geometries. These studies were conducted in parallel with investigations of single crystal Au response and molecular dynamics simulations. IFM measurements of indentation response near steps on an Au <111> surface were used to evaluate the influence of isolated defects on elastic response. Molecular dynamics simulations were performed to model indentation response as a function of applied stress and proximity to defects. In light of the differences between the simulations and experiments, we propose that measurements of thin film elastic response reflect the collective response of the grains and defects such as voids and grain boundaries.

2.0 Experiment

Controlled-probe contact experiments using scanning probe microscopy (SPM) or nanoindentation techniques can be used to measure forces and displacements on the atomic-scale, thereby directly exploring the elastic and plastic deformation of materials at the nanometer level. The IFM, described in detail elsewhere [30], is ideally suited for such mechanical property measurements since it combines the small mechanical loop and imaging capability of an SPM with a stable feedback controlled load sensor for quantitative load-displacement measurements. The force measurements were quantified by measuring the sensitivity of the load sensor (100 μN/V) and the machine compliance (>3000 N/m) using a standard laboratory balance. The displacement measurements were calibrated by using the IFM to image samples with known step heights. The IFM was equipped with a hard piezo and all indentations were performed at a constant displacement rate (10 nm/s) to minimize the effects of piezo non-linearity. It was not necessary to correct any of the load-displacement curves measured in this study for machine compliance or drift (displacement and load drift of less than 0.1 nm/s and 1 nN/s is typical). The IFM was equipped with diamond indenters whose geometry was shaped using a focused ion beam micromachining process described elsewhere [31]. Indenters with a parabolic geometry were used for this study for a predictable contact area - indentation depth relationship which greatly simplifies

the measurement of elastic response. The indenter geometry was measured ex-situ using a scanning electron microscope and in-situ by imaging probe characterizer structures with the IFM.

Measurements of elastic response were performed on Au thin film systems commonly used as interconnects for GaAs devices. 100 nm thick Au films (on 10 nm of Cr or Ti) were prepared by e-beam evaporation (1 nm/sec) onto 25 C Si substrates. The Si substrates were HF dipped before being placed into the evaporation chamber (10^{-6} torr) and then Argon sputtered for 30 sec before deposition(s). Previous analysis of these films suggests a columnar, or "bamboo", grain structure and a predominately <111> texture. The in-plane grain size (average diameter) varies from 50 nm at the surface of the film to about 10 nm at the substrate. A grain diameter of 25 nm will be used for all subsequent calculations reflecting an average of the in-plane grain size. The out of plane grain size is the same as the film thickness (100 nm). It is worth emphasizing that these films were not deposited near the equilibrium conditions for film growth and are therefore expected to be highly defected and associated with large residual stresses [1,2,11-17].

The residual and applied stress-states of these films were inferred from laser deflection and interferometric measurements of wafer curvature. The residual stress of the Au/Cr/Si and Au/Ti/Si samples was measured to be 100±25 MPa tensile and 50±25 MPa compressive, respectively. These values clearly reflect the average stress-field conditions of the films as large grain to grain variations have been demonstrated [1-3,11,13,15,17,32].

Au single crystal surfaces oriented in the <111> direction were prepared to study the influence of isolated defects on nanoindentation measurements. These samples were prepared by a standard technique in which high purity (99.99%) Au wires are flame annealed to form faceted balls [33]. After preparation the facet surfaces are defect free and are characterized by wide terraces (100-250 nm) separated by individual and multiple steps.

The Au thin film and bulk samples were piranha cleaned, placed in a 0.5 mM solution of hexadecanethiol [$CH_3(CH_2)_{15}SH$] in ethanol for 12 hours, and then ethanol rinsed before measurement. The self-assembling alkane-thiol passivates the chemical and adhesive interactions between the indenter and Au [34] which simplifies the analysis of load-displacement curves. The alkane-thiol layer also minimizes the adsorption of water and contamination on the sample's surface while the experiments are being conducted.

A concentric ring bending device, shown in Fig. 1, was used to controllably vary the biaxial stress-state of a film from 50 MPa compressive to 50 MPa tensile with a ±10 MPa uncertainty. Fracture of the Si substrate prohibits the application of higher stresses. The stress applied to the thin film is found using Eq. 1 (Stoney's equation) where R_s is the

radius of the curvature applied by bending which was measured by interferometery. The thickness of the substrate is given by t_s and E_f and ν_f are the elastic modulus and Poisson's ratio of the film, respectively. In this way IFM measurements of elastic properties can be correlated directly with the applied stress, while the morphology of the film and adhesion to the substrate remain constant. Measurements of wafer curvature before and after applying stress indicate that the residual stress state of the samples was unaffected by changes in applied stress.

3.0 Analysis

For the work presented in this paper, a Hertzian model [18,35] was used to analyze the initial response of the thin films to loading, thereby determining the properties of the samples without first plastically deforming them. This approach ensures that the measurements are insensitive to the formation of pile-up or sink-in and also minimizes their sensitivity to substrate effects which scale with indentation depth [36]. Application of the Hertzian contact model requires a quantitative measurement of the force-distance relationship and the indenter geometry and also assumes a linear-elastic response of the sample with no adhesion (no chemical interactions between the indenter and the surface). The elasticity of the indenter-Au contact was confirmed by the lack of hysterisis in the load-displacement curves (for measurements to peak loads of less than 3 μN) and by comparing the images acquired before and after indentation. A study of surface response with and without the monolayer indicates that the presence of the passivating layer causes the load response to deviate slightly from that of an uncoated surface for indentation depths of less than 0.8 nm.

If the requirements stated above are met, the relationship between load and deformation closely follows the classical Hertzian model for a rigid, non-interacting parabolic punch deforming an elastic half space stated by Eq. 2. This equation relates the initial loading response of a surface to the reduced elastic modulus E*. $E^* = (1-\nu_i)/E_i + (1-\nu_s)/E_s$, and E_i, E_s and ν_i and ν_s are the indenter and sample moduli and Poisson's ratios, respectively. The indentation depth, d, is controlled using the z-piezo of the IFM, and the indenter's radius of curvature, R, is measured independently as stated above. The force acting on the indenter, F, is continuously measured by the IFM load sensor [30]. Eq. 2 can therefore be fit to the initial loading response to determine the measured elastic modulus.

4.0 Results

4.1 Measured elastic response depends upon applied stress

The sensitivity of the Au thin film's elastic response to applied stress, measured one week after deposition, is illustrated by the loading portions of three load-displacement curves (plotted on the same axes) in Fig. 2. The measurements were acquired by indenting a R=100 nm diamond indenter into a 100 nm thick Au/Cr/Si sample clamped in the concentric ring bending device. Fig. 2 shows the force acting on the diamond plotted as a function of z-piezo position for three different applied stress conditions. Since the curvature of the diamond indenter is greater than the average grain diameter these measurements reflect the 'average' response of several grains. The loading response of the thin film in the unstressed case is shown by the dotted line. The loading response while compressive (tensile) stress was applied is shown as the dashed (broken) line. The Hertzian fits used to determine the effective elastic moduli from these measurements are shown as the solid lines. The point at which the measured data deviates from the Hertzian fits indicates the onset of plasticity. The dependence of the film's initial loading response upon applied stress can be observed by comparing these curves. When a compressive stress is applied to the film the load increases more rapidly with displacement (dashed line) than in the unstressed (dotted) case. With a tensile stress applied, the load increases less rapidly (broken) than in the unstressed (dotted) case. This difference in initial loading response reflects a change in the film's measured elastic response. The change was quantified by using the Hertzian fit (solid lines) to obtain a measured modulus from each load-displacement curve. A value of $E = 68\pm2$ GPa ($E = 34\pm2$ GPa) was measured with compressive (tensile) stress applied while $E = 48\pm2$ GPa was measured for the unstressed case. The uncertainties listed with measured moduli reflect the fitting uncertainty.

The sensitivity of elastic response to applied stress, measured on several films one week after deposition, is summarized in Fig. 3. This figure illustrates the repeatability and reversibility of the dependence of elastic response upon applied stress. Each data point represents an average of the moduli obtained from seven load-displacement curves, measured at different places on the sample, for a particular applied stress condition. The y-axis error bars are the standard deviation of the moduli measured for each condition. The x-axis error bars reflect the uncertainty of the applied stress values. Every data point is labeled with a number which indicates its position in a measurement sequence. For example, data point 1 represents the average elastic response measured for the first applied stress condition: unstressed. Data point 2 reflects the measurements from the second set of load curves of the sequence, made on the same Au/Cr/Si sample with 5 ± 10 MPa stress applied. The solid line ties together the entire sequence of measurements (1-8) performed

on this sample. The elastic response measured with the sample unstressed, mounted on the IFM stage, is shown by points 1, 5 and 8. Within experimental uncertainties, the same response is measured with the sample unstressed as when less than 10 MPa of stress is applied (2,4,7). From this observation we conclude that using the wafer bending device does not significantly change the measurement compliance and bias the results. The response of the film when compressive (tensile) stress is applied is consistently above (below) the averaged unstressed response as shown by data point 3 (6). This measurement sequence (points 1-8) illustrates that the change in measured elastic response with applied stress is reversible. The response of the film before applying stress (1) is the same as after applying stress (5). Two additional experiments were performed to test the repeatability of this dependence. The dashed line represents data from a similar measurement sequence (points 1-3 in Fig. 3) performed on the same Au/Cr/Si sample. The dotted line represents data from another measurement sequence (points *1-3* in Fig. 3) performed on a Au/Ti/Si sample. These data sets confirm that the observed dependence is repeatable and that it is not unique to one particular Au thin film.

4.2 Measured elastic response depends upon thermal history

The dependence of measured elastic response on applied stress is plotted as a function of a film's thermal history in Fig. 4. This figure summarizes measurements performed on one Au/Cr/Si film within a week of deposition, six months after deposition and then after a low temperature anneal. The sensitivity measured one week after deposition is shown as a solid line (corresponding to points 1-8 in Fig. 3). The measured elastic modulus increased to 65±6 GPa with applied compressive stress (50±10 MPa) and decreased to 32±9 GPa with applied tensile stress (-50±10 MPa) while the unstressed response was 47±6 GPa. The same film's sensitivity six months after deposition is shown by the broken line, with a variation from 49±3 GPa for applied compressive to 41±5 GPa for applied tensile and 45±4 GPa unstressed. Measurements performed after the film was subjected to a low temperature anneal (250 C for 1 hour in an N_2 ambient) are summarized by the dashed line. The sensitivity of the response to applied stress changed sign while its magnitude dramatically increased. The measured elastic modulus decreased to 51±4 GPa with applied compressive stress and increased to 79±9 GPa with applied tensile while the unstressed response was 68±8 GPa. Measurements of wafer curvature before and after annealing indicate that the residual stress relaxed from -100±25 MPa tensile to -50±25 MPa tensile as a result of the anneal.

4.3 Measurements of elastic response depend upon the ratio of grain to indenter size

The point to point variation of the measured elastic response was found to depend critically on the ratio of the indenter curvature to the grain diameter. The standard deviation of the measured modulus values is plotted as a function of the indenters' radius of curvature in Fig. 5. For indenters characterized by curvatures a factor of five greater than the average grain diameter (R>100 nm) the measured modulus values were found to vary less than a ±6 GPa from point to point. At the opposite extreme, for indenters with curvatures a factor of two smaller than the grain diameter, measured modulus values varied as much as a factor of 2 from point to point resulting in standard deviations of greater than 21 GPa. Unreasonably large changes in contact area (>8x) would be required to explain such point to point variations (see Eq. 2) suggesting that the origin of this variation is mechanical. Images acquired before and after indentation indicate that the measured elastic response varies on the same scale as the grain boundary structure.

4.4 Measured elastic response varies near isolated defects

IFM indentations performed near isolated defects on Au <111> surfaces [33] highlight the correlation of indentation elasticity and defect structure. The measured elastic modulus around a isolated surface step on an Au <111> surface was found to repeatably vary from 68±1 GPa on the up-step to 72±1 GPa on the down-step as shown in Fig. 6. This variation extends out from a step more than one indenter diameter indicating that the effect is not due to changes in the indenter - surface contact area. A measured elastic modulus value of 70±2 GPa, consistent with the literature values for bulk samples, was recorded on the wide terraces separating the surface steps. The variation near steps sharply contrasts the consistency of IFM indentation measurements performed on defect free surfaces (point to point variations of less than ±1 GPa are typical when measuring defect free Si <100> surfaces).

4.5 Molecular dynamics simulations of nanoindentation

The experimental studies presented here have been conducted in parallel with molecular dynamics simulations of nanoindentation. Shenderova et al. performed simulations in which a nanoscale tip was used to indent a <111> oriented Au lattice subjected to external strains [37]. They documented a 11-13% change of indentation modulus for very high strains (±7%). In these simulations the indentation modulus was found to increase with applied compressive stress and decrease with applied tensile stress. A similar sensitivity of modulus of applied stress was observed in simulations performed by Kelchner et al [38]. In separate studies, simulations of indentation near step edges have been performed by Kelchner et al [39] and Shenderova et al [40]. Results of these

simulations suggest that modulus values should vary on the order of the ratio of applied stress to the bulk modulus (less than 2%) and that this variation should extend less than one diameter of the indenter from a step edge. The variation of measured modulus with stress state and near defects is at least an order of magnitude less than was observed in the experiments reported here. It should be noted that scaling differences (indenter curvature) between the simulations and experiments make direct comparison difficult. However an increase in the indenter radius used in the simulations would increase the deformation zone [18,35,36] and thereby increase the range of the effect while decreasing its magnitude. The differences between the simulations and experiments suggest that the presence of defects introduces an additional compliance that is not accounted for in the simulations.

5.0 Discussion

The results reported here demonstrate that measurements of elastic response are dependent on the defect structure and stress state in a way that cannot be explained by conventional models of elasticity. The sensitivity of elastic response to applied stress in the Au films is at least an order of magnitude larger than observed for coarse-grained bulk samples [28] and in simulations of defect free Au <111> [37,38]. The variation of indentation response with applied stress, near grain boundaries and across surface steps cannot be explained solely by changes in elasticity due to bond compliance. Similarly the change in elastic properties with low temperature annealing cannot be explained by the conventional model of elasticity. The measured elastic properties must therefore reflect a composite response due to both a bond and defect compliance. If the defect structures provide a nonlinear contribution to the compliance and this is coupled with a nonlinear lattice compliance (conventional elasticity), then it is not entirely surprising that the measured elastic response is also nonlinear and therefore appears Hertzian. In the following, we propose that the measured elastic properties of these thin metallic films reflect an additional compliance resulting from stress concentration at defects such as voids and grain boundaries.

5.1 Conventional elastic theory

The widely accepted model of elastic properties governed bond geometries and interatomic potentials cannot explain the sensitivity of measured elastic response to stress state reported here. The conventional model ties a material's elastic modulus to the curvature of its interatomic potential and bond density. Based on this model, only slight variations in elastic response with applied stress are expected since the curvature of the interatomic potential does not vary significantly until the bonds are stretched near their

elastic limit. Measurements of elastic response would be expected to vary only 5-10% near the elastic limit (lattice strains approaching 2%) and no measurable variation would be expected for low strain values (less than 0.2%). This prediction agrees with the molecular dynamics simulations outlined above [37,38] but is inconsistent with the results shown in Fig. 2 and 3. The conventional model of elasticity also does not predict a dependence of elasticity upon the thermal history of a material (shown in Fig. 4) unless changes in the bond structure or the interatomic potential occur with thermal cycling.

5.2 Additional compliance due to stress concentration at defects

Several models have been developed to explain how defect related stress concentrations cause the elastic properties of nanocrystalline materials to differ from those of similar coarse-grained materials [6,20,21]. These models treat local changes in the interatomic spacing [20] or pore geometry [6,21], caused by stress concentration, as a source of additional compliance. However, the sensitivity of an additional defect compliance to applied stress has not been accounted for in these descriptions. Furthermore the dependence of defect compliance upon the thermal history of a material has not been explained using these descriptions. The existing models of defect dependent elasticity must be re-evaluated in light of these new findings. In the following, the observed sensitivity of elastic modulus to stress state and thermal history is discussed in terms of the effect of grain boundaries and voids upon the measured elastic properties.

5.3 Grain boundaries as a source of additional compliance

Grain boundaries have been identified as a source of unusual elastic and plastic (super-plasticity) properties in nanocrystalline materials. Recent large scale molecular dynamics simulations suggest that grain boundaries of thin metallic films can be characterized by much lower elastic constants (order of magnitude) than perfect crystals [41]. These simulations suggest that thin film strain is accommodated largely at grain boundaries resulting in a dramatic increase in the interatomic spacing and a corresponding decrease in the elastic constants. Some experimental studies (Au, Cu, Se, Pd, Mg and CaF_2) support this hypothesis [9,10,20,24] and a few even suggest that the grain boundaries may be associated with interatomic potentials different than those of a perfect crystal [20]. Other studies (Fe, Cu, Ni) do not support the notion of grain boundary dependent elastic properties [4]. These contradictory results may be reconciled by noting the differences in how the samples were prepared.

The effect of grain boundaries on the measured elastic properties can be estimated using the mixture rules for composite materials (lower bound Eq. 3 and an upper bound

Eq. 4 [20]). E_{tot} is the measured modulus, E_{gb} and E_{cystal} are the moduli for the intercrystalline and crystal components with volume fractions V_{gb} and $V_{crystal}$ respectively. V_{gb} is given by Eq. 5 assuming an average grain boundary diameter d, a tetrakaidecahedron grain shape and a grain boundary thickness given by Δ. Assuming d=25 nm, Δ=1 nm, $E_{crystal}$ = 70 GPa (the Au<111> value) and using the measured (as deposited) value E_{tot} = 47 GPa, the elastic modulus of the grain boundary component is calculated to be in the range of E_{gb} = 14 GPa to -122 GPa. The non-physical negative value is calculated from the lower bound estimate (Eq. 3). The small V_{gb} = 0.12 value requires that the grain boundaries exhibit very different mechanical properties than those of the grains to account for the measured E_{tot} value. Low values of E_{gb} are plausible for the Au films used in this study given that the deposition conditions are likely to result in under-dense grain boundaries [11-17,41]. The change in measured modulus with applied stress reported here requires E_{gb} = 14 GPa to change to E_{gb} = 6.4 GPa with applied tensile stress to explain the observed variation of E_{tot} from 47 to 32 GPa (using the generous upper-bound, Eq. 4). Such a softening in the grain boundary stiffness, E_{gb}, due to an applied tensile stress is consistent with stress concentration at the grain boundaries [41]. Changes in E_{gb} with thermal history are also plausible due to the high diffusivity of grain boundaries. However the change in sign of the sensitivity of the elastic properties to an applied stress, with a low temperature anneal (as shown in Fig. 4), cannot be explained using this model.

5.4 Voids as a source of additional compliance

An alternative explanation for the observed sensitivity of measured elastic response to an applied stress is that the void structures present in the Au films are highly sensitive to an applied stress. This assumption is reasonable considering that the applied stress fields are likely to interact with the void structures causing them to change shape in an effort to minimize the thin film strain. The stress concentration of voids is well documented [11-17], and it is therefore plausible that even small changes in applied stress would effect the shape of the voids and therefore also the measured elastic response. The effect of two types void structures (horizontally and vertically aligned) with differing responses to applied stress, is shown schematically in Fig. 7. Fig. 7(a) shows how an applied compressive stress might cause the vertical voids to close while causing horizontal voids to expand as compared to the unstressed case (Fig. 7(b)). Conversely, an applied tensile stress could cause the vertical voids to expand while causing the horizontal voids to close as shown in Fig. 7(c). The response of individual voids is dependent upon many factors including their surface crystallography and orientation and Fig. 7 is only intended as a

greatly simplified illustration. If horizontal and vertical voids are present in equal proportions then no net change in subsurface free volume would result and the average measured elastic properties would not change. However if there are more vertical voids than horizontal voids, an applied tensile stress would result in a net increase in subsurface free volume and therefore a reduction in the measured elastic modulus. The variation of the measured elastic response with applied stress shown in Fig. 3 can be qualitatively explained using this model if it is assumed that an unequal distribution of vertical voids and horizontal voids are present in these films after deposition. This model can also be used to explain the dependence of measured elastic properties upon thermal history. Annealing is known to cause changes in the sizes and orientations of voids and would therefore change the sensitivity of the films elastic properties to an applied stress.

An empirical dependence of elasticity upon pore volume fraction has been known for some time. More recently Krstic and Erikson proposed a model explaining the origin of this effect [6,21]. They suggested that a full characterization of a porous solid must include the pore size, R, and an inherent flaw size, S, emanating from the surface of the pore as shown in Fig. 8. This shape is plausible as a description for the interface between a void and a grain boundary in the Au thin films. Krstic and Erikson's model predicts that the behavior of a crack opening under an external load, and the interaction of the crack tip stress field with the stress concentration of the pore are responsible for the elastic behavior of a porous solid. Their solutions suggest that the presence of a pore can increase the stress concentration at the crack tip by as much as a factor of three [6,21]. This porosity model can be adapted to explain the observed sensitivity of modulus to stress if it assumed that the applied stress changes the S/R ratio of the voids in the Au thin films. Using the calculations of Krstic and Erikson [21], the porosity model could explain the change in modulus from 47±4 GPa to 33±2 GPa observed in Fig. 3 if a -50 MPa applied tensile stress causes the S/R ratio to increase from 1.1 to 1.9. The porosity model was developed for large (mircon scale) pores and its application on the nanometer scale can be tested to first order using the well-known expression for the stress intensity factor given by Eq. 6. K_c is the fracture toughness, σ is the stress acting on the crack, a is the crack length and f is the geometry factor (ranging from 1 to 10 for a thick or thin sample, respectively). This expression can be used to estimate the conditions required for crack growth given the voids, cracks and stress-state of the Au films. Given a = 25 nm (equal to the grain size) and σ = 250 MPa (3x the applied + residual stress, an upper bound) a grain boundary fracture toughness as low as 0.07 to 0.7 GPa would be required to advance a crack and change the void geometry. These K_c values are roughly a factor of 100 lower than the

fracture toughness values measured on bulk gold samples. This estimate suggests that grain boundaries with dramatically different plastic properties are required in order for Krstic and Erikson's model to apply. It should be noted that the validity of the stress intensity factor has not yet been tested on these length scales. An additional consideration is that changes in the stress state of a film are also known to drive diffusive mechanisms and cause void shape change [11-17]. Time dependent studies are underway to estimate the contribution of such non-dislocation mechanisms.

5.5 Elasticity due to the collective response of grains, grain boundaries and voids

The existing models of grain boundary and void dependent elasticity due not offer a satisfactory explanation of the sensitivity of thin film elasticity to stress state which is reported here. This is not entirely surprising given that such simple models cannot address the complex of the mechanical behavior observed for these films. Previous studies revealed that both inter-grain sliding and intra-grain deformation can accommodate an indenter during nanoindentation [8]. Recent work suggests that the threshold and magnitude of grain slip is effected by the stress state of the films, as will be described in a forthcoming publication [42]. This observation demonstrates that the mechanisms accommodating plastic deformation are highly sensitive to the properties of voids and grain boundarie and may provide an important clue about the origin of the interdependence elastic properties, defect structures and stress state. Given that the plastic deformation (at low loads) proceeds by cooperative grain boundary sliding and grain rotation it is conceivable that the elastic response of the films is also due to the cooperative motion of grains. The elastic energy stored in the contact is likely to be preferentially stored in the form of local grain boundary and void deformations and only to a lesser degree in the deformation of the grains themselves. This deformation preference is driven by the stress concentrations and lower elastic constants of the grain boundary and void regions. Changes in the thin film stress state would also alter the defect compliance preferentially and therefore effect the measured elastic response. The point to point variation in the measured elastic properties (shown in Fig. 5) is consistent with local variations in this cooperative elasticity. Annealing induced changes in the void and grain boundary structures alters the super-plastic behavior [42] and would therefore also result in changes in the cooperative elasticity. A complex interaction of multiple grains, grain boundaries and voids appears to be responsible for the elastic properties of the Au thin films.

6.0 Conclusions

A dependence of measured elastic response upon defect structure has been demonstrated using nanoindentation. The sensitivity of measured elastic modulus to applied stress reported here suggests a new method for probing the local stress state and defect structures of thin metallic films. Analysis of experiments and simulations reveals that the defect properties of these films are responsible for their unique elastic properties. Indentation measurements of elastic response appear to reflect the cooperative deformation of grains, voids and grain boundaries. Changes in the distribution of defect sizes and orientations with time and temperature underlie the dependence of this sensitivity upon thermal history. We conclude that the elastic properties of thin metal films are critically dependent upon their deposition conditions, thermal histories and stress states. Furthermore, the elastic response of these films varies on the same scale as their defect structure. In summary, measurements of thin film elastic response reflect a composite elasticity comprised of both bond and defect compliance. These results have wide ranging implications for measuring and modeling the behavior of metallic thin films such as those used as interconnects in integrated circuits. Transmission electron microscopy techniques and time dependent indentation studies are now underway to further our understanding of the link between defect structure, stress and elastic response in hopes of providing the foundation for establishing nanoindentation as a technique for the highly localized measurement of thin film stress state.

ACKNOWLEDGMENTS

The authors are greatly indebted to Don Brenner, Olga Shenderova, and Jim Mewkill at North Carolina State University for their modeling efforts. The authors would furthermore like to acknowledge the folks at Digital Instruments, in particular Jeff Elings, for instrumentation support, Carolyn Matzke at Sandia National Laboratories for her sensor fabrication, and Terry Stark at Materials Analysis Services for his focused ion beam work. The work done at North Carolina State University and at Sandia, which is a multiprogram laboratory operated by Sandia Corporation--a Lockheed Martin Company, was supported by the United States Department of Energy under Contract DE-AC04-94AL85000.

FIGURES

1. Concentric ring bending device
2. Load-Displacement curves for three applied stress conditions
3. Dependence of elastic loading response upon applied stress
4. Dependence of elastic loading response upon applied stress vs. thermal history

5. Point to point variation as a function of indenter radius

6. Modulus vs. step proximity

7. Thin film x-section: applied stress

8. Schematic illustration of spherical pore with annular flaw emanating from its surface

EQUATIONS

1. Stoney's equation for curvature vs. stress

2. Hertzian deformation

3. Lower Limit - Modulus of Grain Boundaries

4. Upper Limit - Modulus of Grain Boundaries

5. Volume fraction of grain boundaries

6. Stress intensity factor

REFERENCES

1. "Stress and grain growth in thin films," C.V. Thompson, R. Carel, J. Mech. Phys. Solids, Vol 44 No 5 (1996) 657.

2. "Size effects in materials due to microstructural and dimensional constraints: a comparative review," E. Arzt, Acta Mater. 46 (1998) 5611.

3. "Grain Size effects in nanocrystalline materials," C. Suryanarayana, D. Mukhopadhyay, S.N. Patankar, F.H. Froes, J. Mater. Res. Vol 7 No 8 (Aug1992) 2114.

4. "On the elastic moduli of nanocrystalline Fe, Cu, Ni and Cu-Ni alloys prepared by mechanical milling/alloying," T.D. Shen, C.C. Koch, T.Y. Tsui, G.M. Pharr, J. Mater. Res., Vol 10 No 11 (1995) 2892.

5. "Mechanical properties of compositionally modulated Au-Ni thin films: Nanoindentation and microcantilever deflection experiments," S.P. Baker, W.D. Nix, J. Mater. Res., Vol 9 No 12 (1994) 3131.

6. "Effect of porosity on Young's modulus of nanocrystalline materials," V. Krstic, U. Erb, G. Palumbo, Scripta Metall. Mater. 29 (1993) 1501.

7. "Superplastic behavior of fine-grained Mg-9Li material at low homologous temperature," E.M. Taleff, O.A. Ruano, J. Wolfenstine, O.D. Sherby, J. Mater. Res., Vol 7 No 8 (1992) 2131.

8. "Nanometer-scale mechanics of gold films," P. Tangyunyong, R.C. Thomas, J.E. Houston, T.A. Michalske, R.M. Crooks, A.J. Howard, Phys. Rev. Lett. Vol 71 No 20 (1993) 3319.

9. "Mechanical behavior of high-density nanocrystalline gold prepared by gas deposition method," S.Sakai, H. Tanimoto, H. Mizubayashi, Acta Mater. 47 (1999) 211.

10. "Grain size dependence of mechanical properties in nanocrystalline selenium," K. Lu, H.Y. Zhang, Y. Zhong, H.,J. Fecht, J. Mater. Res. 12 (1997) 923.

11. "Measurement and interpretation of strain relaxation in passivated Al-0.5% Cu lines," P.R. Besser, T.N. Marieb, Jin Lee, P.A. Flinn, John C. Bravman, J. Mater. Res., Vol 11 No 1 (1996) 184.

12. "Size and volume distributions of thermally induced stress voids in AlCu metallization," S. Kordic, Jan Engel, R.A.M. Wolters, Appl. Phys. Lett. Vol 68 No 8 (1996) 1060.

13. "Effects of mechanical stress on electromigration-driven transgranular void dynamics in passivated metallic thin films," M. R. Gungor, D. Maroudas, L.J. Gray, Appl. Phys. Lett. 73 (1998) 3848.

14. "Electromigration damage and failure distributions in Al - 4 wt % Cu interconnects," W.C. Shih, A.L. Greer, J. Appl. Phys. 84 (1998) 2251.

15. "Electromigration failure by shape change of voids in bamboo lines," E. Arzt, O. Kraft, W.D. Nix, J.E. Sanchez, J. Appl. Phys. 76 (1994) 1563

16. "In situ transmission electron microscopy study of plastic deformation and stress-induced voiding in Al-Cu interconnects," D. Jawarani, H. Kawasaki, I. -S. Yeo, L. Rabenberg, J.P. Stark, P.S. Ho, J. Appl. Phys. 82 (1997) 1563.

17. "Stresses, deformation, and void nucleation in locally debonded metal interconnects," Y.-L. Shen, J. App. Phys. 84 (1998) 5525.

18. S.P. Timoshenko and J.N. Goodier, *Theory of Elasticity* (McGraw-Hill, New York 1970), 3rd ed.

19. "Nanoindentation of Ag/Ni multilayered thin films," J.A. Ruud, T.R. Jervis, F. Spaepen, J. Appl. Phys., Vol 10 No 75 (1994) 4969

20. D. Korn, A. Morsch, R. Birringer, W. Arnold, H. Gleiter, J. de Phys., Coll. C5, Suppl. au no. 10, 49, (1988), C5-769.

21. "A model for the porosity dependence of Young's modulus in brittle solids based on crack opening displacement," V.D. Krstic, W.H. Erickson, J. Mat. Sci., 22 (1987) 2881.

22. "Nanoindentation of nanocystalline ZnO," M.J. Mayo, R.W. Siegel, Y.X. Liao, W.D. Nix, J. Mater. Res., Vol 7 No 4 (1992) 973.

23. "Residual stress measurements of thin aluminum metallizations by continuous indentation and x-ray stress measurement techniques," W.R. LaFontaine, C.A. Paszkiet, M.A. Korhonen, Che-Yu Li, J. Mater. Res., Vol 6 No 10 (1991) 2084.

24. "Mechanical behavior of nanocrystalline Cu and Pd," G.W. Nieman, J.R. Weertman, R.W. Siegel, J. Mater. Res., Vol 6 No 5 (1991) 1012.

25. "Near-plastic threshold indentation and the residual stress in thin films," J.E. Houston, T.A. Michalske, Symposium Mater. Res. Soc., Pittsburgh PA (1997) xv+542, 3.

26. "The effect of stress on the nanomechanical properties of Au surfaces," J.E. Houston, Symposium Mater. Res. Soc., Pittsburgh PA (1997) xii+509, 177.

27. "A new method for estimating residual stresses by instrumented sharp indentation," S. Suresh, A.E. Giannakopoulos, Acta Mater. 46 (1998) 5755.

28. "Influences of stress on the measurement of mechanical properties using nanindentation: Part I. Experimental studies in an aluminum alloy," T.Y. Tsui, W.C. Oliver, G.M. Pharr, J. Mater. Res. Vol 11 No 3 (Mar1996) 752.

29. "Influences of stress on the measurement of mechanical properties using nanoindentation: Part II: Finite element simulations," A. Bolshakov, W.C. Oliver, G.M. Pharr, J. Mater. Res. Vol 11 No 3 (Mar1996) 760.

30. "A new force sensor incorporating force-feedback control for interfacial force microscopy," Joyce, S.A., Houston, J.E., Rev. Sci. Instrum. 62 (1991) 710.

31. "Chemically and Geometrically Enhanced Focused Ion Beam Micromachining," P.E. Russell, T.J. Stark, D.P. Griffis, J.R. Phillips, K.F. Jarausch, JVST B 16 (1998), 2494.

32. "Grain Size-Internal Stress Relationship in Iron-Nickel Alloy Electrodeposits" F. Czerwinski, J. Electrochem. Soc., Vol 143 No 10 (1996) 3327.

33. "Effect of surface steps on the plastic threshold in nanoindentation," J.D. Kiley, R.Q. Hwang, J.E. Houston, Phys. Rev. Lett. Vol 81 No 20 (1998) 4424.

34. "The mechanical response of gold substrates passivated by self-assembling monolayer films," R.C. Thomas, J.E. Houston, T.A. Michalske, R.M. Crooks, Science 259 (1993) 1883.

35. K.L. Johnson, *Contact Mechanics* (Cambridge University Press, Cambridge England 1996).

36. "A study of the mechanics of microindentation using finite elements," T.A. Laursen, J.C. Simo, J. Mater. Res. Vol 7 No 3 (Mar 1992) 618.

37. "An evaluation of atomic force microscopy as a probe of nanoscale residual stress via atomistic simulation," O. Shenderova, J. Mewkill, P. Linehan, D.W. Brenner, K. Jarausch, P.E. Russell, to appear in MRS bulliten: Spring MRS'98 proccedings.

38. Private communication, C.L. Kelchner, J.C. Hamilton.

39. Ibid. (Private communicaton, , C.L. Kelchner, J.C. Hamilton)

40. Private communication, O. Shenderova, J. Mewkill, D.W. Brenner.

41. "Molecular-dynamics study of copper with defects under strain," P. Heino, H. Häkkinen, K. Kaski, Phys. Rev. B 58 (1998) 641.

42. "Room temperature super-plasticity of Au interconnect films," K.F. Jarausch, J.E. Houston, P.E. Russell, in preperation.

EQUATIONS

$$\sigma_f = \frac{t_s \, E_f}{2 \, R_s \, (1 - \nu_f)} \qquad (1)$$

$$F = \tfrac{4}{3} E^* \, (R^{\frac{1}{2}}) \, d^{\frac{3}{2}} \qquad (2)$$

Lower Limit: $$E_{tot} = V_{gb} \, E_{gb} + V_{cryst} \, E_{cryst} \qquad (3)$$

Upper Limit: $$E_{tot} = \frac{E_{gb} \, E_{cryst}}{V_{gb} \, E_{cryst} + V_{cryst} \, E_{gb}} \qquad (4)$$

$$V_{gb} = 1 - \left(\frac{d - \Delta}{d}\right)^3 \qquad (5)$$

$$K_c = f \sigma \sqrt{\pi a} \qquad (6)$$

FIGURES

Figure 1. Schematic illustration of the concentric ring bending device used to apply stress (either tensile or compressive) to the interconnect films during a nanoindentation measurement. Note that the applied curvature is greatly exaggerated.

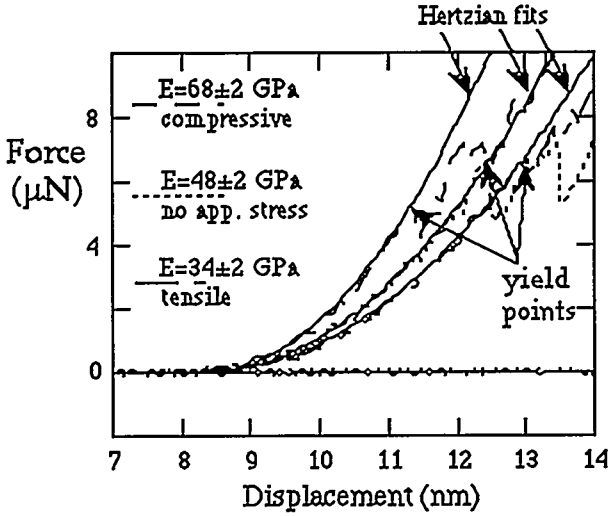

Figure 2. Three load-displacement curves which illustrate the effect of applied stress upon the elastic loading response of an Au interconnect film (note that only the initial loading portions of the load-displacement curves are shown). The effective elastic modulus values were determined from each curve using the Hertzian fits (solid lines).

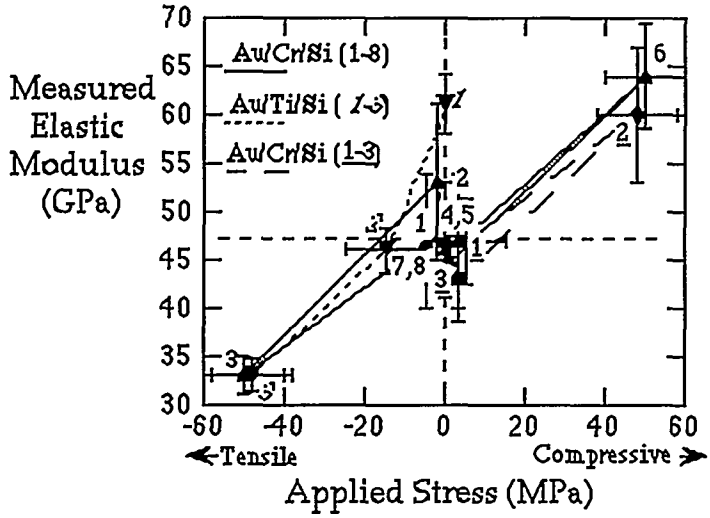

Figure 3. The measured elastic response plotted as a function of applied stress for Au interconnect films. Each data point represents an average of seven load-displacement curves (obtained at different points on the film) for each stress condition, and the order of each measurement sequence is indicated by the accompanying numbers.

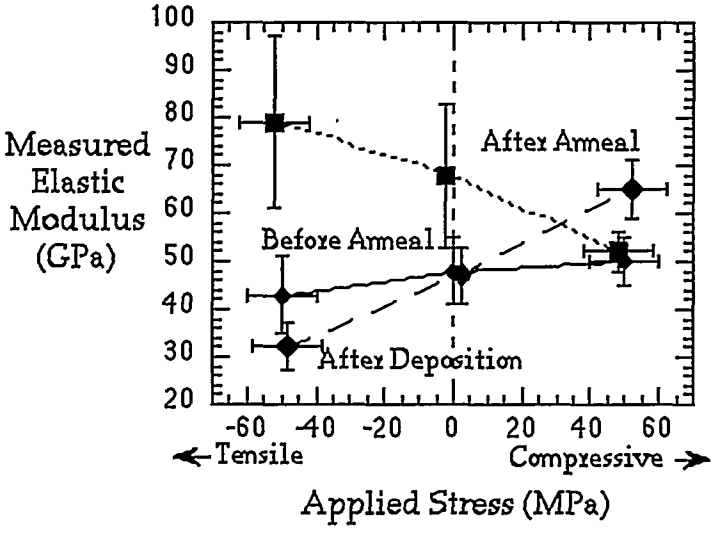

Figure 4. The sensitivity of the measured elastic modulus to an applied stress after deposition (dashed line), six months after deposition (solid line) and then after six months and an anneal (dotted line). Each data point represents at least 20 load-displacement curves.

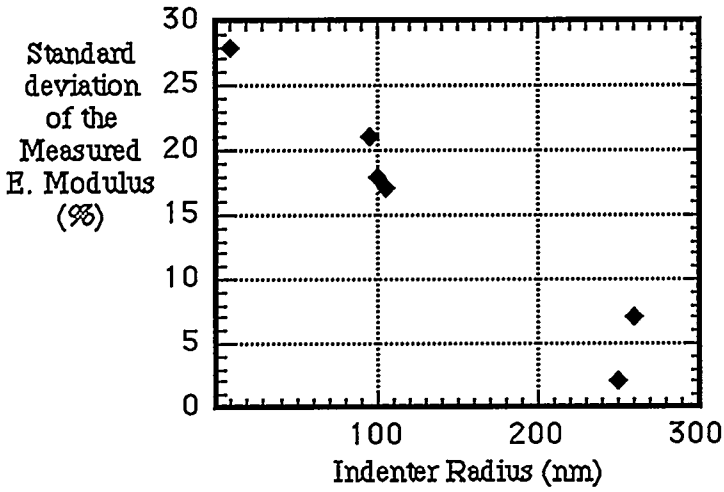

Figure 5. The point to point variation of the measured elastic modulus as a function of the indenter radius (the average grain diameter is 25 nm). Each data point represents the standard deviation for 20 load-displacement curves.

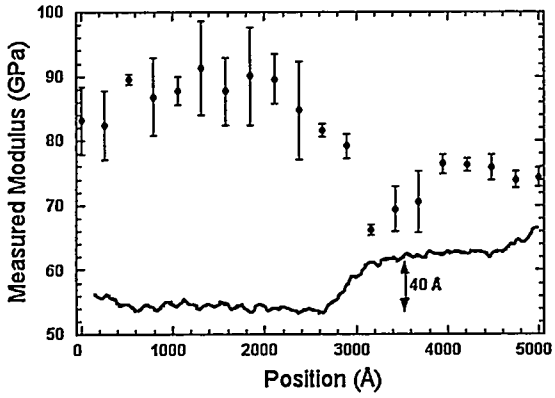

Figure 6. Measured elastic modulus as a function of position relative to a step on an Au <111> surface.

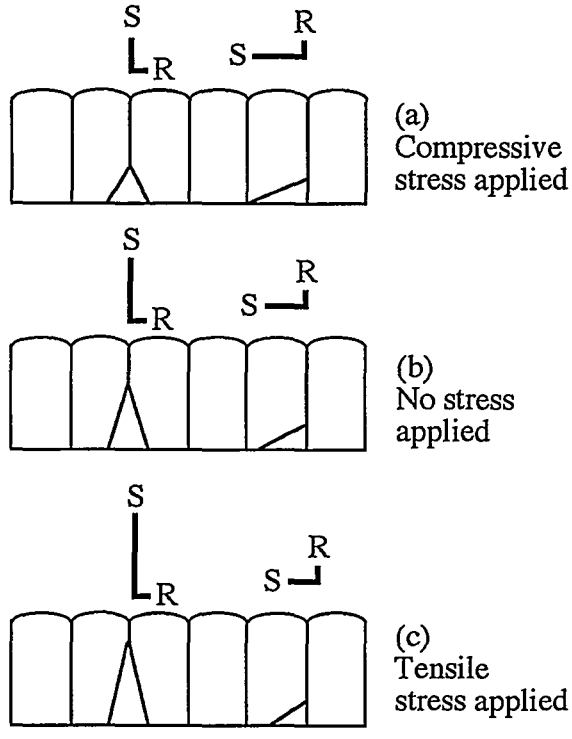

Figure 7. Schematic illustration of changes in void shape and size with applied compressive stress (a), no applied stress (b), and applied tensile stress (c). Note that the size of the voids is greatly exaggerated for the sake of illustration.

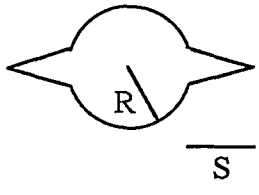

Figure 8. Spherical pore or void with annular flaws emanating from its surface.